ResearchGate

See discussions, stats, and author profiles for this publication at: https://www.researchgate.net/publication/321503938

A Fluid-Particle Interaction Method for the Simulation of Particle-Laden Fluid Problems

Conference Paper · January 2017

DOI: 10.20906/CPS/CILAMCE2017-0139

CITATIONS
3

READS
4,702

4 authors:

Ana Carolina da Silva Fernandes
University of São Paulo
2 PUBLICATIONS **4** CITATIONS
SEE PROFILE

Henrique Campelo Gomes
University of São Paulo
9 PUBLICATIONS **21** CITATIONS
SEE PROFILE

Eduardo M. B. Campello
University of São Paulo
58 PUBLICATIONS **688** CITATIONS
SEE PROFILE

Paulo M Pimenta
University of São Paulo
117 PUBLICATIONS **1,683** CITATIONS
SEE PROFILE

All content following this page was uploaded by Eduardo M. B. Campello on 12 December 2017.

The user has requested enhancement of the downloaded file.

A FLUID-PARTICLE INTERACTION METHOD FOR THE SIMULATION OF PARTICLE-LADEN FLUID PROBLEMS

Ana Carolina S. Fernandes

Henrique C. Gomes

Eduardo M. B. Campello

Paulo M. Pimenta

casf@usp.br

henrique.campelo@usp.br

campello@usp.br

ppimenta@usp.br

Polytechnic School at the University of São Paulo

Av. Prof. Luciano Gualberto, cross 3, nº 380, 05508-010, São Paulo, SP, Brazil

Abstract. *This work proposes a new method for solving coupled problems of fluid mechanics and discrete particle mechanics. The idea is based on previous works by (Gomes and Pimenta 2015) and (E. de M. B. Campello 2016), and the goal is to develop an efficient computational model suited to simulate problems involving flowing fluid media laden with solid particles. We are especially interested in the simulation of percolation flow through porous media. The fluid problem is resolved by a standard finite element approach using local element velocity-pressure pairs satisfying the LBB compatibility condition, with the resulting nonlinear system of equations being iteratively solved by the Newton-Raphson method. As an important feature, the fluid mesh remains fixed during the flow, just as in classical Eulerian approaches, and its interface conditions with the (nonmatching) particles´ boundaries are imposed through discontinuous piecewise constant Lagrange multipliers interpolating functions. An implicit, staggered interactive and iterative scheme is adopted to achieve convergence within each time step. The particles´ problem, in turn, is resolved in a discrete element approach, wherein both grain-to-grain and grain-to-wall (fixed boundaries) contacts are fully permitted and resolved. The influence of the fluid on the motion of the particles is represented by means of forces, which are computed from the fluid flow and imposed on the particles in a coupled, iterative way. In order to illustrate the potentialities of the proposed scheme, steady and unsteady flow simulations are presented.*

Keywords: *Finite Element Method, Fluid-Particles Interaction, Discrete Element Method, Embedded Interfaces*

INTRODUCTION

In Engineering as a whole, there are several activities concerning granular materials immersed in fluids, such as oil well drillings in submerged rocks using rotating drills and the fluid percolation through porous media (e.g., the soil). The higher the viscosity of the fluid media and the contact surface between the fluid and the grains, more meaningful are the efforts generated by the flow around the solid.

The fluid and granular material interaction realistic simulation depends on the coupled systems resolution, i.e., it depends on the simultaneous resolution of two interdependent domains, which are Discrete Particle Mechanics and Fluid Mechanics. To do so, complex models that require robuster and more powerful processors to be calculated are made necessary.

The granular materials physics, which describes the particles set mechanical behavior through the particle-particle interaction, started to be simulated by computer methods known as Particle Methods, among which the most notorious are: the Discrete Element Method (DEM), used in this document, the Molecular Dynamics Methods and the Smoothed Particle Hydrodynamics Method.

The artifice used in this article to study the Fluid-Particle interaction is based on the concepts and techniques already stablished in the Fluid-Structure Interaction (FSI) area. In this line of research, computational simulation software are being developed with different formulations, in an attempt to solve problems such as the self-excited vibrations, effects such as flutter, free surfaces in contact with the structure, turbulent flows, and so on. However, each method is more efficient for a determined situation, due to the existent peculiarities.

In this article, a study on the Fluid-Particle Interaction problems is presented, as well as the methods and formulations used to solve them. Further on, a program code capable of simulating particle-laden fluids will be developed from program formulations previously designed by (Gomes and Pimenta 2015) and (E. de M. B. Campello 2016). The software with the two previously mentioned works combination will be tested by simulating some basic Fluid-Particle Interaction problems.

1. FLUID-PARTICLE INTERACTION

Granular materials are abundant found and used in different fields of human activities. They may be either in their natural form, such as grains of sand, snow flakes and atmospheric dust, or in classes of materials produced specially for specific applications, such as concrete fillers and additives, powder or grain food, and fine grain compact aggregates of high added value for the chemical, pharmaceutical and microelectronics industries. Nevertheless, the human knowledge about the granular materials physics is still restricted and technologically underused.

In many cases, the granular material is found immerse in fluid media that is more viscous than the atmospheric gases and, therefore, the effect caused by these media on the particle movement, when friction, drag and sustaining forces are applied, become significant and shall be considered in the kinematic studies. Some examples in which the fluid-particle interaction is considerable for the physical phenomenon understanding are the oil well drillings in submerged rocks using rotating drills, where there is disaggregation and fragmentation of rocky

material and the fluid percolation through porous media (e.g., the soil), process of great importance in civil engineering construction works.

As demonstrated above, there are several activities concerning the fluid-particle interaction that are expensive, dangerous and that present a high technological complexity, so that the computational simulation of these problems before the real operation execution is extremely necessary. However, this interaction generates problems known as coupled systems, which require the simultaneous resolution of two interdependent domains: the Discrete Particle Mechanics and the Fluid Mechanics. The latter is a nonlinear dynamic problem, which implicates solving Complex Partial Derivatives Differential Equations. That is, finding the system solution in which the interface boundary conditions between fluid and granular material are unknown and dependent of this solution is a very difficult task and, therefore, requires sophisticated and optimized models to be simulated and calculated.

With previous works as a baseline, such as (Gomes 2013), which approaches the Mechanical of Fluids and the Fluid-Structure Interaction (FSI), and (E. de M. B. Campello 2016), which addresses the Discrete Mechanical of Particles, it is possible for a new method to be developed in order to fluid-particle interactions coupled problems to be solved. The idea is to consider the solid particles as "structures" and to use the formulations that are widely studied and applied in FSI, together with adaptations that encompass the particle physics formulations, as shown later on in this article.

2. NUMERICAL METHODS FOR THE FLUIDS PROBLEM SOLVING

Currently, the most prominent methods to solve FSI problems can be divided into two groups, according to the manner they approach the interface between the solid and the fluid. The Coincident Boundaries Method is the one where the mesh of fluid elements ends where the mesh of structure elements begins, and the nodes located on the boundary between both meshes belong to both domains (Figure 1 (a)). This method is elaborated by means of an ALE (Arbitrary Lagrangian Eulerian) approach, in which the fluid is formulated and solved by the deformation that its mesh sustains when keeping up with the structure mesh movement.

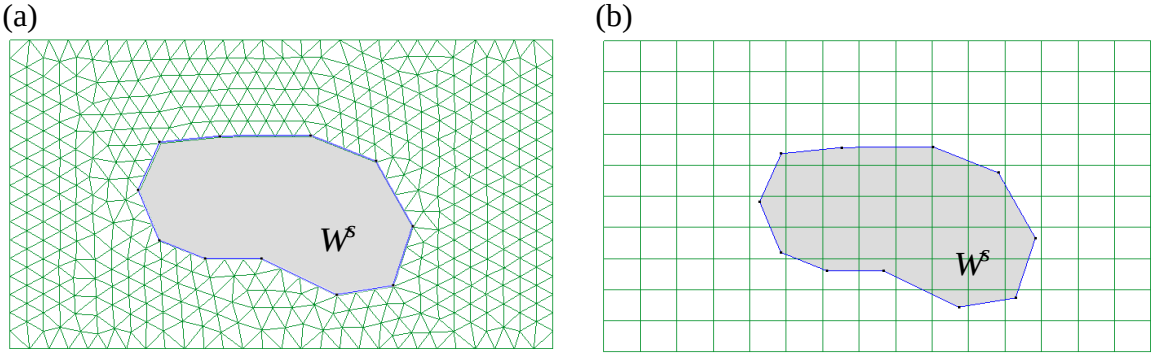

Figure 1 - (a) Coincident boundary. (b) Immersed boundary.

The other group is the Immersed Boundaries Method. In this case, both the meshes of the fluid and of the structure are independent and overlapped (Figure 1 (b)). The fluid can be solved by means of a classical Eulerian approach in which the mesh is fixed and non-deformable, very suitable characteristics that avoid the excessive distortion of the elements in this domain. The solid is solved the usual way, using the Lagrangian approach. An application of this technique

to a blade immersed in fluid flow with continuous rotation problem, published in (Gomes and Pimenta 2015), can be seen in the Figure 3. In Figure 2, the both fluid and structure meshes are shown, using the Immersed Boundaries technique.

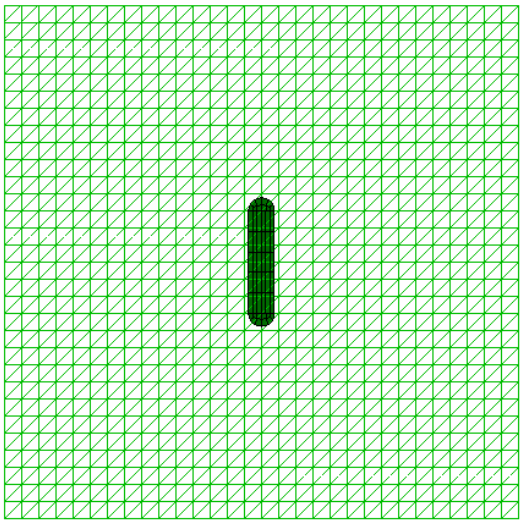

Figure 2 –Structure and fluid meshes in a blade with continuous rotation problem.

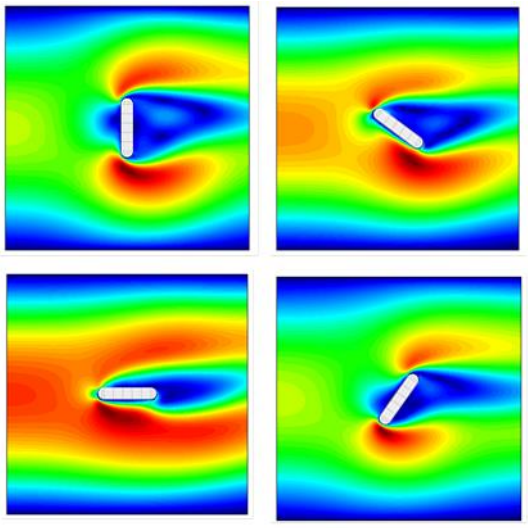

Figure 3 – Color map of the velocities field.

Despite solving the problem of fluid elements distortion, in order for the Immersed Boundaries Method to be used, it is necessary that some technique enforcing the displacements from the structure in the interface region into the fluid to be implemented, as these displacements are boundary condition for the solving of the fluid. However, there are no fluid mesh nodes in the border region of the solid to avoid that some nodes of different meshes merge after the structure movement. Therefore, the displacement effects cannot be passed to the fluid in a trivial manner, and its boundary conditions must be translated as imposed velocities, what typifies a boundary condition of Dirichlet type (Gomes 2013).

There are some ongoing studies concerning manners for the imposition of velocities to the fluid in FSI tridimensional problems. One of them consists in using a formulation that combines the Generalized Finite Element Method (GFEM) with the Lagrange Multipliers. As follows, we will examine the formulation developed to solve the fluid problem.

2.1 Eulerian fluids approach

Before the fluid flow study is initiated, some considerations about the real physical problem are necessary. An important observation is that, although the fluids are compressible, it is possible to consider the flow as incompressible, provided that the implicated velocities are low enough.

The basic equations of mass conservation and fluid momentum (Donea and Huerta 2003) will be referred to, in their differential and integral forms, and they will be the basis of the subsequent mathematical development.

Mass Conservation. According to Newton`s Laws, the mass (m) of a certain material volume should be maintained over time (t). Referring only to incompressible flows, in which the fluid

density do not vary over time and neither in space, and after some mathematical manipulation, the mass conservation equation is as follows:

$$\frac{dm}{dt} = 0 \rightarrow \frac{d}{dt}\int_V \rho \, dV = 0 \rightarrow \text{div}\, \boldsymbol{v} = 0 \tag{1}$$

where ρ is the fluid density, V is the referred material volume, and $\boldsymbol{v}$ is the velocity of the material on spots over the control surface.

Momentum Conservation. The momentum equation is given by the correlation between the momentum ($\boldsymbol{Q}$) variation of a certain material volume with the time and the sum of acting forces over that volume. Using the mass conservation equation and the momentum variation over time, it can be written as follows:

$$\frac{d\boldsymbol{Q}}{dt} = \frac{d}{dt}\int_V \rho \boldsymbol{v} \, dV = \int_V \overbrace{d\boldsymbol{v}/dt}^{aceleration} \; \overbrace{\rho \, dV}^{mass} \tag{2}$$

Adding to the equation the volume and surface forces that act over the fluid volume:

$$\rho \, d\boldsymbol{v}/dt = \underbrace{\rho \boldsymbol{b}}_{\substack{volume \\ forces}} + \underbrace{\text{div}\, \boldsymbol{T}}_{\substack{surface \\ forces}} \leftrightarrow \rho \underbrace{\partial \boldsymbol{v}/\partial t}_{\substack{local \\ aceleration}} + \rho \underbrace{(\nabla \boldsymbol{v})\boldsymbol{v}}_{\substack{convective \\ aceleration}} = \rho \boldsymbol{b} + \text{div}\, \boldsymbol{T} \tag{3}$$

where $\boldsymbol{b}$ is the volume force divided by the fluid mass, and $\boldsymbol{T}$ are the Cauchy Stress in each surface element.

Navier-Stokes Equations. For Newtonian fluids incompressible flows, the Cauchy Stress Tensor and its divergent are as follows:

$$\boldsymbol{T} = -\bar{p}\boldsymbol{I} + 2\mu\varepsilon(\boldsymbol{v}) \qquad \text{div}\, \boldsymbol{T} = -\nabla\bar{p} + 2\mu \, \text{div}(\nabla^S \boldsymbol{v}) \tag{4}$$

$$\mu = \nu \, \rho \qquad \bar{p} = p \, \rho \qquad \varepsilon(\boldsymbol{v}) = {}^1/_2 \, (\nabla \boldsymbol{v} + (\nabla \boldsymbol{v})^T) \tag{5}$$

where μ is the fluid dynamics viscosity, ν s the kinematic viscosity, $\bar{p}$ is the pressure, p is the kinematic pressure, $\varepsilon(\boldsymbol{v})$ is the velocity strain rate tensor, and $\nabla^S \boldsymbol{v}$ is the velocity symmetrical gradient, which is equal to the strain rate tensor.

For the first equation of Navier-Stokes to be obtained, the expression of div $\boldsymbol{T}$ shall be substituted in the momentum conservation equation, resulting in:

$$\dot{\boldsymbol{v}} + (\nabla \boldsymbol{v})\boldsymbol{v} - 2\nu \, \text{div}(\nabla^S \boldsymbol{v}) + \nabla p = \boldsymbol{b} \tag{6}$$

In order to obtain the complete Navier-Stokes Equations, a system of differential partial equations, it is still necessary that the initial conditions are imposed, as well as the Essential (Dirichlet) and Natural (Neumann) boundary conditions. Therefore, the 5 equations that form the Navier-Stokes Equations deducted in the 19th Century are:

$$\left.\begin{cases} \dot{\boldsymbol{v}} + (\nabla \boldsymbol{v})\boldsymbol{v} - 2\nu \operatorname{div}(\nabla^{\mathrm{S}}\boldsymbol{v}) + \nabla p = \boldsymbol{b} \\ \operatorname{div} \boldsymbol{v} = 0 \\ \boldsymbol{v} = \boldsymbol{v}_0 \ , \quad on\ time = 0 \end{cases}\right\} \ on\ \Omega$$
$$\begin{cases} \boldsymbol{v} = \overline{\boldsymbol{v}} \ , \quad on\ \Gamma_u \\ (2\nu\varepsilon(\boldsymbol{v}) - p\boldsymbol{I})\boldsymbol{n} = \bar{\boldsymbol{t}} \ , \quad on\ \Gamma_t \end{cases} \tag{7}$$

where $\overline{\boldsymbol{v}}$ is the prescribed velocity, $\bar{\boldsymbol{t}}$ is the prescribed traction, Ω is the problem domain, Γ_u is the contour part where the Essential B.C. are imposed and Γ_t is the part where the Natural B.C. are imposed.

Weak Form. In order for the Navier-Stokes equations weak form to be found, it is necessary to choose arbitrary functions $\boldsymbol{w} \in \mathcal{H}_1(\Omega)$ and $q \in \mathbb{L}_2(\Omega)$ for the velocities and pressure test functions, respectively. The Navier-Stokes partial differential equations system can be rewritten in the integral form as:

$$\int_\Omega \boldsymbol{w} \cdot \dot{\boldsymbol{v}}\, d\Omega + \underbrace{\int_\Omega \boldsymbol{w} \cdot (\nabla \boldsymbol{v})\boldsymbol{v}\, d\Omega}_{\boldsymbol{convective\ term}} - \underbrace{\int_\Omega \boldsymbol{w} \cdot 2\nu \operatorname{div}(\nabla^S \boldsymbol{v})\, d\Omega}_{\boldsymbol{viscous\ term}} + \underbrace{\int_\Omega \boldsymbol{w} \cdot \nabla p\, d\Omega}_{\boldsymbol{pressure\ term}}$$
$$= \int_\Omega \boldsymbol{w} \cdot \boldsymbol{b}\, d\Omega \tag{8}$$
$$\int_\Omega q \cdot \operatorname{div} \boldsymbol{v}\, d\Omega = 0$$

Integrating by parts the viscous and pressure terms and using a compact notation where $\int_{\mathrm{X}} Y \cdot Z\, dX = (Y, Z)_{\mathrm{X}}$, the weak form of the problem is stated as:

$$(\boldsymbol{w}, \dot{\boldsymbol{v}})_\Omega + c(\boldsymbol{v}; \boldsymbol{w}, \boldsymbol{v})_\Omega + a(\boldsymbol{v}, \boldsymbol{w})_\Omega - (\operatorname{div} \boldsymbol{w}, p)_\Omega + (q, \operatorname{div} \boldsymbol{v})_\Omega - (\boldsymbol{w}, \bar{\boldsymbol{t}})_{\Gamma_t}$$
$$= (\boldsymbol{w}, \boldsymbol{b})_\Omega \tag{9}$$
$$\forall\ (\boldsymbol{w}, q) \in \boldsymbol{\mathcal{V}} \times \mathcal{Q}$$

where $c(\boldsymbol{v}; \boldsymbol{w}, \boldsymbol{v})_\Omega = \int_\Omega \boldsymbol{w} \cdot (\nabla \boldsymbol{v})\boldsymbol{v}\, d\Omega$ and $a(\boldsymbol{v}, \boldsymbol{w})_\Omega = \int_\Omega 2\nu\, \nabla^S \boldsymbol{w} : \nabla^S \boldsymbol{v}\, d\Omega$**.** For the problem to be solved, it is necessary that $\boldsymbol{v}(x,t) \in \boldsymbol{\mathcal{S}} \times]0,T]$ and $p(x,t) \in \mathcal{Q} \times]0,T]$ can be found and satisfy the above stated equation.

2.2 Newmark`s method for time integration

It is possible to determine the fluid acceleration on the next time step t^{n+1} as follows:

$$\dot{\boldsymbol{v}}^{n+1} = \frac{1}{\gamma}\frac{(\boldsymbol{v}^{n+1} - \boldsymbol{v}^n)}{\Delta t} - \frac{(1-\gamma)}{\gamma}\dot{\boldsymbol{v}}^n \tag{10}$$

where $\dot{\boldsymbol{v}}^n$ is the current step time acceleration and γ is the Newmark integration parameter.

Newmark`s Method is considered implicit, i.e., the value of the desired variable on the time step $n+1$ depends on that same value. The Navier-Stokes equation system discretized over time by means of this method, presented on weak form, is stated as:

$$\{(\boldsymbol{w},\boldsymbol{v})_\Omega + \gamma\Delta t[c(\boldsymbol{v};\boldsymbol{w},\boldsymbol{v})_\Omega + a(\boldsymbol{v},\boldsymbol{w})_\Omega - (\operatorname{div}\boldsymbol{w},\mathrm{p})_\Omega + (q,\operatorname{div}\boldsymbol{v})_\Omega - (\boldsymbol{w},\boldsymbol{b})_\Omega - (\boldsymbol{w},\bar{\boldsymbol{t}})_{\Gamma_t}]\}^{n+1} = (\boldsymbol{w},\boldsymbol{v}^n)_\Omega + (1-\gamma)\Delta t(\boldsymbol{w},\dot{\boldsymbol{v}}^n)_\Omega \quad (11)$$

$\forall\ (\boldsymbol{w},q) \in \boldsymbol{\mathcal{V}} \times \mathcal{Q}$

2.3 Space discretization by finite elements

As we already know the Navier-Stokes equations, it is possible to infer that the velocity and the pressure are primitive problem variables, and this makes us choose a mixed finite element for the discretization. Besides, the pressures field can be interpreted as Lagrange Multipliers, however, in order to avoid numerical instabilities, it is necessary that the finite element satisfies the "LBB" condition of velocity/pressure, i.e., it should present less degrees of liberty for pressure and more degrees of liberty for velocity.

In this work, we will use a triangular finite element known as P2P1, as the velocities are interpolated by compatible quadratic functions, and the pressures, by linear incompatible functions. Figure 4 shows that the pressures are calculated just on the triangle vertexes, while the velocities are calculated on the vertexes and on the midpoints of the sides.

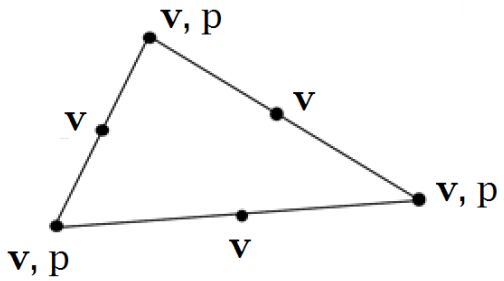

Figure 4 - P2P1 Element

For the space discretization to be made, it is necessary that the approximation $(\boldsymbol{v},p)$ and weight $(\boldsymbol{w},q)$ functions are substituted by their approximations, described below:

$$\begin{matrix} approximations \\ of\ approximation \\ function \end{matrix} \begin{cases} \boldsymbol{v}^h(x) = \bigcup_{e=1}^{N_{el}} \mathbf{N}_v\ \mathbf{v}_e \\ p^h(x) = \bigcup_{e=1}^{N_{el}} \mathbf{N}_p\ \mathbf{p}_e \end{cases} \quad \begin{matrix} approximations \\ of\ weight \\ function \end{matrix} \begin{cases} \boldsymbol{w}^h(x) = \bigcup_{e=1}^{N_{el}} \mathbf{N}_v\ \mathbf{w}_e \\ q^h(x) = \bigcup_{e=1}^{N_{el}} \mathbf{N}_p\ \mathbf{q}_e \end{cases} \quad (12)$$

where N_{el} is the number of finite elements used for discretization, h is the function approximation indication, e indicates local domain nodal values, and N_v and N_p are form functions matrices.

After substitution and certain mathematical work, the system can be written in matrix form, which represents the fluid in a global manner:

$$\begin{bmatrix} \dfrac{\mathbf{M}}{\gamma\Delta t} + (\,\mathbf{C}(\boldsymbol{v}^{n+1}) + \mathbf{K}) & \mathbf{G} \\ \mathbf{G}^T & 0 \end{bmatrix} \begin{Bmatrix} \mathbf{v}^{n+1} \\ \mathbf{p}^{n+1} \end{Bmatrix} = \begin{Bmatrix} \mathbf{f}^{n+1} + \dfrac{\mathbf{M}}{\gamma\Delta t}\mathbf{v}^n + \dfrac{(1-\gamma)}{\gamma}\mathbf{M}\dot{\mathbf{v}}^n \\ 0 \end{Bmatrix} \tag{13}$$

where $\mathbf{M}$ is the mass matrix, $\mathbf{C}$ is the convective matrix, $\mathbf{K}$ is the viscous matrix, $\mathbf{G}$ and $\mathbf{G}^T$ are the gradient and divergent operators, $\mathbf{f}$ is the vector containing the volume forces and applied stresses. All these global terms are the local contributions scattering results, which are not going to be detailed here.

The existence of the convective matrix makes the system nonlinear, in which the solution is bound to the solving of the own obtained system. Therefore, numerical methods are necessary for this resolution. In this work, the Iterative Newton-Raphson Method is applied, consisting of an efficient algorithm capable of determining approximations of function`s squares with root convergence.

2.4 Immersed boundaries

In this work, in order for the coupled FSI problem to be solved, the Immersed Boundaries Method will be adopted, as it allows the fluid to be solved with a fixed Eulerian mesh, following the mathematical formulation shown in the previous section. By definition, we will divide the problem domain in two parts: Ω^s is the structure domain, limited to the space occupied by the solid, and Ω^f is the fluid domain, which, besides the space occupied by itself, also covers the region filled by the solid.

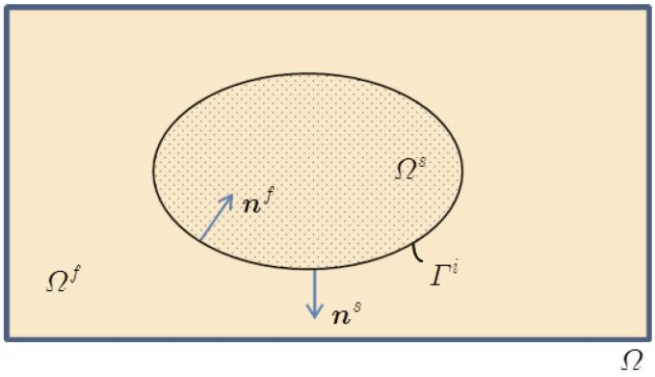

Figure 5 – Domains formed by the decomposition of the fluid domain

The wet surface, in turn, divides the fluid domain in two regions. The first, named Ω^+ is the region filled only by the fluid. The subdomain Ω^- is the region occupied by the solid and known as fictitious domain. In mathematical language, we state:

$$\Omega^+ \cup \Omega^- = \Omega^f \qquad \text{and} \qquad \Omega^+ \cap \Omega^- = \emptyset \tag{14}$$

So that the processing and the memory use can be optimized, the finite elements belonging to the fictitious fluid domain are deactivated during the resolution of the problem. Figure 5 shows the Ω^s and Ω^f domains with their single vectors $\boldsymbol{n}^f$ and $\boldsymbol{n}^s$ normal to the interface Γ^i, also named “wet surface”.

Interface Conditions. There are two conditions that shall be satisfied along the interface between fluid and solid (Eq. (15)). The first of them is an adherence kinematic condition, where the fluid and structure velocities shall be the same. The second is a dynamic condition that estimates the force balance over Γ^i, what can be interpreted as the stresses balance with opposite orientations due to the normal vectors $\boldsymbol{n}^f$ and $\boldsymbol{n}^s$ of each domain:

$$\boldsymbol{v}^f = \boldsymbol{v}^s \quad \forall x \in \Gamma^i \qquad\qquad \boldsymbol{T}^f\boldsymbol{n}^f = -\boldsymbol{T}^s\boldsymbol{n}^s \quad \forall x \in \Gamma^i \tag{15}$$

Moving Interface. One possible way to understand the interaction between fluid and structure is to admit that, if the displacements of the solid are known, the problem is reduced to a fluid with moving interfaces. Therefore, the kinetic and dynamic conditions turn into Essential and Natural Boundary Conditions, respectively, stated as:

$$\boldsymbol{v}^f = \overline{\boldsymbol{v}}^i \quad \forall x \in \Gamma^+ \qquad\qquad \bar{\boldsymbol{t}}^f = \boldsymbol{0} \quad \forall x \in \Gamma^- \tag{16}$$

where $\overline{\boldsymbol{v}}^i$ is the moving interface velocity. Note that the Essential B.C. is imposed only in the approximation of the interface by the Ω^+domain, and the Natural B.C. is imposed in the approximation of the interface by the fictitious Ω^- domain.

In this work, the Essential B.C. (Dirichlet) will be imposed by means of Lagrange Multipliers ($\boldsymbol{\lambda}$). This is a technique that was already used by other authors, such as (Gerstenberger and Wall 2008), (Legay, Chessa, and Belytschko 2006), (Moës, Béchet, and Tourbier 2006) and (Sawada and Tezuka 2010). To this end, it is necessary to define a functional (π) and, later, to calculate the variation of this functional ($\delta\pi$) as follows:

$$\begin{aligned}\pi &= \int_{\Gamma^+} \boldsymbol{\lambda}\cdot\left(\boldsymbol{v}-\overline{\boldsymbol{v}}^i\right)d\Gamma^+ \\ \delta\pi &= \int_{\Gamma^+} \delta\boldsymbol{\lambda}\cdot\left(\boldsymbol{v}-\overline{\boldsymbol{v}}^i\right)d\Gamma^+ + \int_{\Gamma^+} \boldsymbol{\lambda}\cdot\delta\boldsymbol{v}\,d\Gamma^+\end{aligned} \tag{17}$$

It is important to stress that the Lagrange Multipliers physical interpretation, obtained through the dimensional analysis, is a traction acting along the Γ^+ interface, i.e., the traction performed by the fluid in the wet surface. Besides, $\boldsymbol{\lambda}$ becomes an extra problem unknown when this technique is used.

Finally, it is possible for the essential boundary condition in the Navier-Stokes Equations weak form to be introduced, substituting the velocities variation $\delta\boldsymbol{v}$ by the weight function $\boldsymbol{w}$, just so the previous notation is maintained, and the obtained result is:

$$\begin{aligned}\Big\{(\boldsymbol{w},\boldsymbol{v})_{\Omega^{\mathrm{f}}} + \gamma\Delta t\Big[&c(\boldsymbol{v};\boldsymbol{w},\boldsymbol{v})_{\Omega^{\mathrm{f}}} + a(\boldsymbol{v},\boldsymbol{w})_{\Omega^{\mathrm{f}}} - (div\,\boldsymbol{w},\mathrm{p})_{\Omega^{\mathrm{f}}} + (q,div\,\boldsymbol{v})_{\Omega^{\mathrm{f}}} \\ &- (\boldsymbol{w},\boldsymbol{b})_{\Omega^{\mathrm{f}}} - (\boldsymbol{w},\bar{\boldsymbol{t}})_{\Gamma_t} - (\boldsymbol{w},\boldsymbol{\lambda})_{\Gamma^+} - \left(\delta\boldsymbol{\lambda},\boldsymbol{v}-\overline{\boldsymbol{v}}^i\right)_{\Gamma^+}\Big]\Big\}^{n+1} \\ &= (\boldsymbol{w},\boldsymbol{v}^n)_{\Omega^{\mathrm{f}}} + (1-\gamma)\Delta t(\boldsymbol{w},\dot{\boldsymbol{v}}^n)_{\Omega^{\mathrm{f}}}\end{aligned} \tag{18}$$

Interface Discretization. There are several manners to perform the Lagrange Multipliers $\boldsymbol{\lambda}$ discretization and its test function $\delta\boldsymbol{\lambda}$ in the Γ^i interface. One of them, suggested by (Gerstenberger and Wall 2008), is to employ the fluid mesh itself to generate points over the

interface, as can be seen in Figure 6. This way, the form functions use the nodes (triangles) to perform the interpolation and find the $\boldsymbol{\lambda}$ e $\delta\boldsymbol{\lambda}$ approximations, stated as:

$$\boldsymbol{\lambda}^h = \bigcup_{e=1}^{N_{el}} \mathbf{N}_{\boldsymbol{\lambda}}\, \boldsymbol{\lambda}_e \quad \text{and} \quad \delta\boldsymbol{\lambda}^h = \bigcup_{e=1}^{N_{el}} \mathbf{N}_{\boldsymbol{\lambda}}\, \delta\boldsymbol{\lambda}_e \tag{19}$$

where $\mathbf{N}_{\boldsymbol{\lambda}}$ is the form functions matrix, and $\boldsymbol{\lambda}_e$ is the local nodal value.

This manner of discretizing the interface can generate some numerical instability, especially when finite elements with interpolation functions of low order are used in the fluid problem formulation. This instability occurs due to the incompatibility between the Lagrange Multipliers approximation subspace and the velocity and pressure approximation subspaces (LBB), and it was already highlighted in (Gerstenberger and Wall 2008) and (Moës, Béchet, and Tourbier 2006).

Alternatively, this work uses the technique indicated in (Sawada and Tezuka 2010), in which the interface is discretized by a mesh that is independent from the fluid mesh, and together with discontinuous approximation functions for the Lagrange Multipliers interpolation (Figure 7). That way, it is possible to choose any dimension for the $\boldsymbol{\lambda}$ approximation subspace, and the calculation of the terms to be integrated along the interface is facilitated.

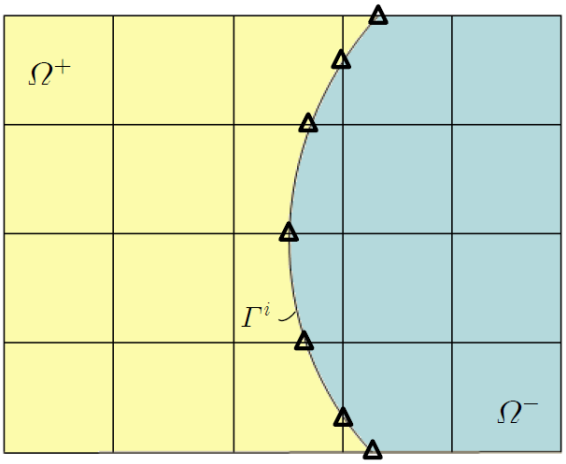

Figure 6 – Interface discretization using the fluid mesh

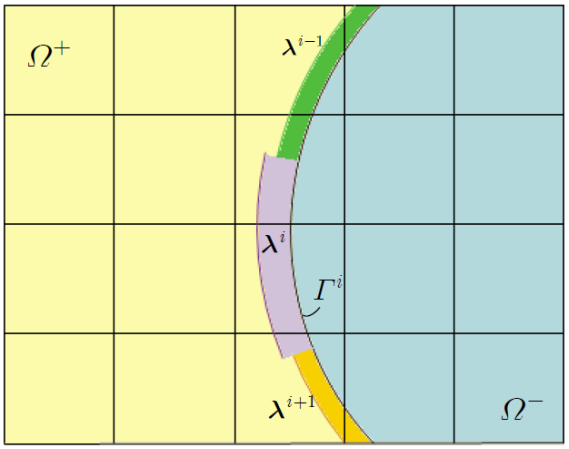

Figure 7 – Interface discretization regardless of the fluid mesh, using discontinuous and constants functions in the interior of the elements

Matrix Problem. Substituting the approximation and weight functions in the weak form expression, and after some mathematical work, it is possible for the system to be written in matrix form, thus representing the problem in a global manner:

$$\begin{bmatrix} \dfrac{\mathbf{M}}{\gamma\Delta t} + (\,\mathbf{C}(\mathbf{v}^{n+1}) + \mathbf{K}) & \mathbf{G} & -\mathbf{M}_{\boldsymbol{\lambda}}^{\mathrm{T}} \\ \mathbf{G}^{\mathrm{T}} & \mathbf{0} & \mathbf{0} \\ -\mathbf{M}_{\boldsymbol{\lambda}} & \mathbf{0} & \mathbf{0} \end{bmatrix} \begin{Bmatrix} \mathbf{v}^{n+1} \\ \mathbf{p}^{n+1} \\ \boldsymbol{\lambda}^{n+1} \end{Bmatrix} = \begin{Bmatrix} \mathbf{f}^{n+1} + \dfrac{\mathbf{M}}{\gamma\Delta t}\mathbf{v}^n + \dfrac{(1-\gamma)}{\gamma}\mathbf{M}\dot{\mathbf{v}}^n \\ \mathbf{0} \\ -\mathbf{M}_{\boldsymbol{\lambda}}\, \bar{\mathbf{v}}^i \end{Bmatrix} \tag{20}$$

where the operator $\mathbf{M}_{\boldsymbol{\lambda}}$ is the Lagrange Multipliers matrix. All of these global terms are the local contributions scattering result, which will not be detailed here.

3. PARTICLE-PARTICLE INTERATION PROBLEMS

There are several types and scales of granular materials, which vary from fine powders and atmospheric dust, passing through the sand grains on a beach, through tons of food grains stored in silos, until reaching the rocky material disaggregation during the drilling of oil wells with drills (Figure 8).

Figure 8 – Examples of granular materials, presenting the distinctions between them. Images: www.freeimages.com, Laura Mattos Fortes e Eduardo M. B. Campello.

When the study object physical phenomenon scale is much bigger than the grains dimension that compose the material, a physic approximation is possible, and the granular set can be dealt with as a unity. This is the way the Geotechnical Engineering problems are studied, for instance. However, when the phenomenon and the granular material scales draw near, it is made necessary to deal with every grain individually, as an elementary solid of determined mass, volume and form, thus forming a discrete media.

One of the greatest difficulties about solving problems that concern granular materials is the way to describe the particle set mechanical behavior, as every grain is different and unique, forming an heterogeneous media that is, several times, multiphasic. As a result, the particle-particle interaction physics started to be simulated by computational methods named as Particle Methods, among which the most notorious are: the Discrete Element Method (DEM), the Molecular Dynamics Methods and the Smoothed Particle Hydrodynamics Method. Some renowned works on the subject are (Cundall and Strack 1979), (Gingold and Monaghan 1977) and (Alder and Wainwright 1959), besides the precious contributions by (Duran 1997), (Pöschel and Schwager 2005), (Crowe et al. 2011), (Zohdi 2007), (Bićanić 2004), (O'Sullivan 2011) and (Wellmann and Wriggers 2011).

Approaching the particle-particle problem by the Discrete Element Method makes it possible for the finite tridimensional rotation movement of a grain to be described by vectors, by means of a second order rotation tensor. This, in turn, can be parameterized and, by limiting

the rotations magnitude between two consecutive configurations, the necessary number of independent parameters is reduced to three, thus making the vector parameterization very suitable for the computational processing, in addition to approximating by resemblance the rotation description to the already known translation movement description (E. M. B. Campello 2015).

Among several techniques to perform the vector parameterization, in this article a special rescaled vector parameterization is adopted, based on the Rotation Vector by (Rodrigues 1840) and (Ibrahimbegovic 1997). As a result, few trigonometric functions with reference to real rotation axes of movement description are obtained. One of the disadvantages of the parameterization is the impossibility to know the exact number of spins that a particle performed in relation to the initial position. However, this information becomes irrelevant for DEM simulations, as only the rotation between two consecutive configurations is needed, and they can be adjusted according to the rotation velocity, in order to avoid complete spins during the time between one and another.

This way, a parameterization with particle rotation movement geometric meaning is possible to be obtained, with relatively low computational costs and a movement description that is similar to the translation.

4. BRIEF DESCRIPTION OF THE DEM MODEL

A set of particles interacting among themselves and with the surrounding media (walls and fluids) can be treated as a discrete dynamical system within a DEM approach. The particles are subjected to a combination of forces as gravity, drag and lift forces, near-field (attractive and repulsive), contact and friction forces, that is responsible to cause translational and rotational motion to them.

The entire deduction of the formulation can be seen in (Neto and Campello 2017). Here, basically are presented the particles motion equations and the acting forces and moments. Imposing Euler´s laws for each particle i at every time instant t, we have:

$$m_i \ddot{\boldsymbol{x}}_i = \boldsymbol{f}_i^{tot} \qquad \text{and} \qquad j_i \dot{\boldsymbol{\omega}}_i = \boldsymbol{m}_i^{tot} \tag{21}$$

where m is the particle mass, $\boldsymbol{x}$ is the position vector, j the rotational inertia, $\boldsymbol{\omega}$ the spin vector, $\boldsymbol{f}^{tot}$ and $\boldsymbol{m}^{tot}$ are the particle total force and total moment vectors (with respect to the particle center). Superposed dot denotes differentiation with respect to time. Particle's motion evolution in time can be found by numerical integration of Eq. (21).

The total force vector is composed by:

$$\boldsymbol{f}_i^{tot} = m_i \boldsymbol{g} + \boldsymbol{f}_i^{nf} + \boldsymbol{f}_i^{con} + \boldsymbol{f}_i^{fric} + \boldsymbol{f}_i^{fluid} \tag{22}$$

where $\boldsymbol{g}$ is the gravity acceleration vector, $\boldsymbol{f}_i^{nf}$ are the forces due to near-field interactions with other particles, $\boldsymbol{f}_i^{con}$ the forces due to mechanical contacts, $\boldsymbol{f}_i^{fric}$ the forces due to friction caused by these contacts and $\boldsymbol{f}_i^{fluid}$ the forces applied by involving fluid as the drag and lift forces.

Almost all these forces are assumed to act only on the particle's center, so, they not contribute to the total moment vector. The exceptions are the eccentric friction and fluid forces, originating the following expression:

$$\boldsymbol{m}_i^{tot} = \boldsymbol{m}_i^{fric} + \boldsymbol{m}_i^{fluid} \tag{23}$$

where $\boldsymbol{m}_i^{fric}$ is the moment generated by the friction forces and $\boldsymbol{m}_i^{fluid}$, the moment generated by fluid forces.

5. THE RESULTS SO FAR

The research practical part is under development and, so far, a simpler software is in use, which describes only the fluid by the Finite Element Method for stationary and transient (dynamics) problems.

Subsequently, a software that simulates the interaction with solids by means of the Immersed Boundaries will be used and, finally, the formulation developed by (E. de M. B. Campello 2016) for particle-particle interaction will be attached, resulting in a software capable of solving Fluid-Particle problems.

5.1 Stationary problems

Flow around a Cylinder. This problem simulates a 2,2m long and 0,41m wide narrow pipeline, and origin of the coordinate system in the left inferior vertex. There is a fluid flow from the left to the right, passing by a 0,05m radius cylinder, centered in (0,2;0,2)m, which works as an obstacle for the fluid. On the lateral walls of the pipeline, the velocity is null, and the exit of the right corner is considered an open boundary with null applied traction.

The horizontal flow velocity in the entrance of the pipeline is parabolic and described as:

$$v(0, x_2) = \left[\frac{4U_m x_2 (H - x_2)}{H^2} \quad 0\right]^T \tag{24}$$

with the vector position $x = x_i e_i$, width of the pipeline H and maximum entrance velocity U_m. This way, the average velocity, the Reynolds number and the Strouhal number are stated as:

$$\bar{U} = \frac{2v\left(0, \frac{H}{2}\right)}{3} \quad , \quad Re = \frac{\bar{U}D}{\nu} \quad e \quad St = \frac{fD}{\bar{U}} \tag{25}$$

where D is the cylinder diameter, f is the frequency of the vortex detachment [s-1] and ν is the kinematic viscosity of the fluid.

The parameters adopted for this problem were:

$$\rho[kg/m^3] = 1 \quad , \quad \nu[m^2/s] = 1 \times 10^{-3} \quad , \quad U_m[m/s] = 0{,}3 \quad , \quad Re = 20 \tag{26}$$

The results of the simulation are stated below:

a)

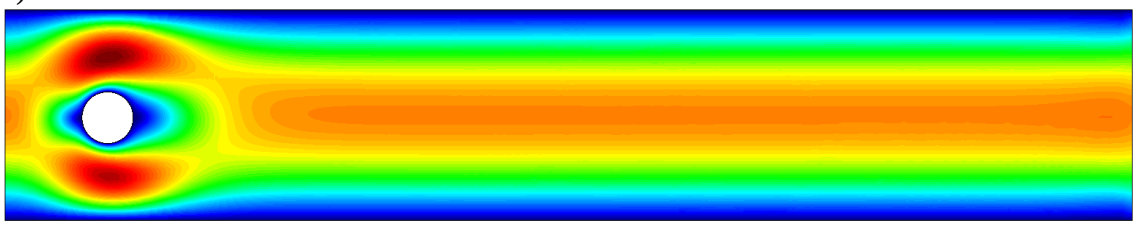

b)

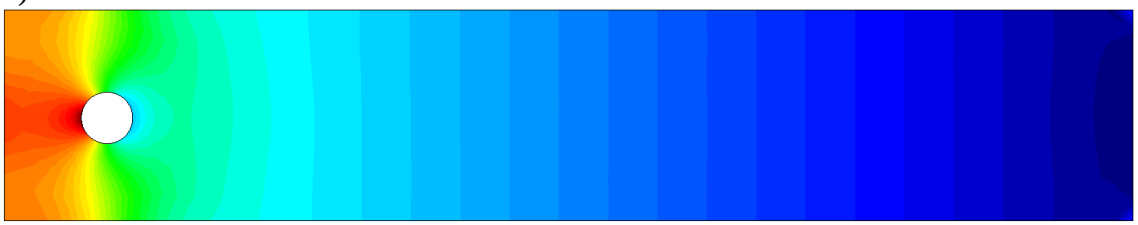

Figure 9 – Flow velocities (a) and pressure (b) fields. The warmer the colors are, the bigger are the values.

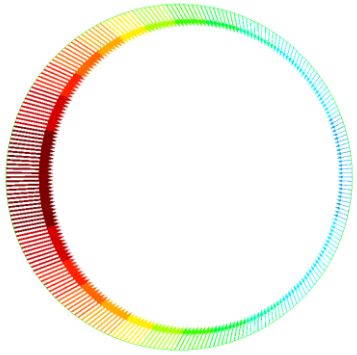

Figure 10 – Traction vectors in the cylinder caused by the flow.

Cavity flow. The second problem simulates a square cavity with side equal to 1 meter, filled with fluid. In the superior side, a constant horizontal velocity of 1 m/s is imposed, from the left to the right, thus generating flow inside the cavity. On the vertical walls and on the bottom of the reservoir, the fluid velocity is null.

In this case, the Reynolds number is as follows:

$$Re = \frac{v_h L}{\nu} \tag{27}$$

where v_h is the imposed horizontal velocity, L is the dimension of the cavity side and ν is the kinematic viscosity of the fluid equal to 1m²/s. I.e., the Reynolds number is unitary for this equation.

Some results are shown as follows:

a) b)

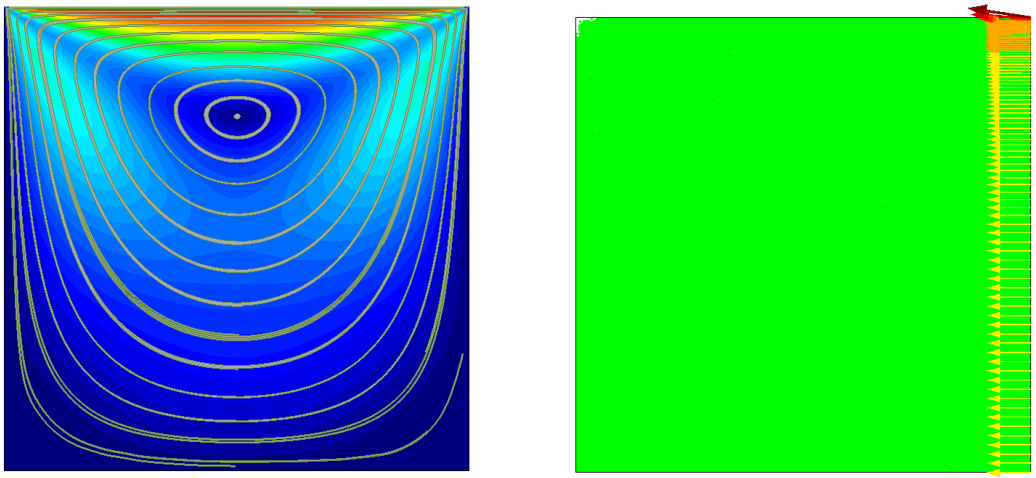

Figure 11 – Velocity fields with flow lines (a) and traction vectors concentrated on internal right side (b)

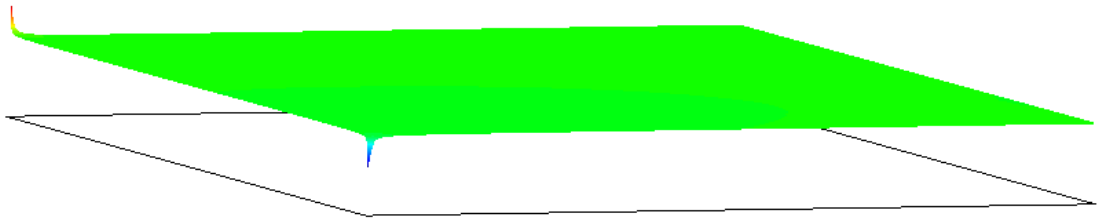

Figure 12 – Pressure concentration singularity in the superior vertexes of the cavity. View of the pressure in surfaces.

Flow in a pipeline with section reduction. At last, there is a problem to consider, which simulates a pipeline with the exactly same geometrical characteristics of the previously mentioned problem "Flow around a Cylinder". The flow also occurs from the left to the right, but there is a reduction of the section, due to a 0,15m high "step", located 1 meter distant from the flow entry and working as an obstacle for the fluid.

The horizontal velocity flow in the pipeline entrance is parabolic and has the same parameters specified in the "Flow around a Cylinder" problem, except for the kinematic velocity $\nu = 2 \times 10^{-4}$, which generates a higher Reynolds number, equal to 100.

The following images show some of the obtained results:

a)

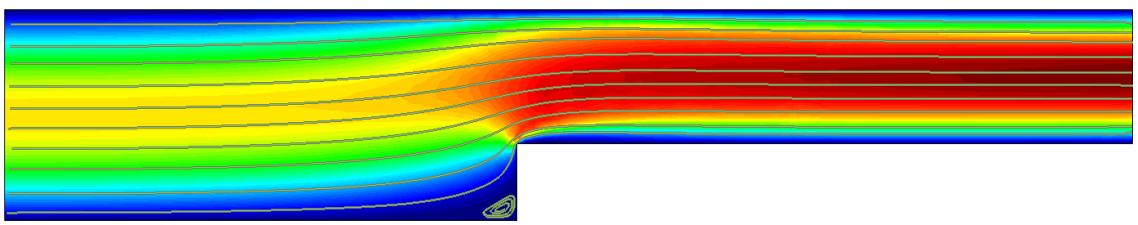

b)

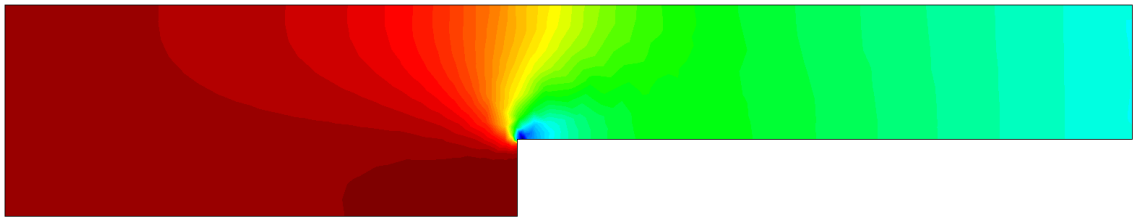

c)

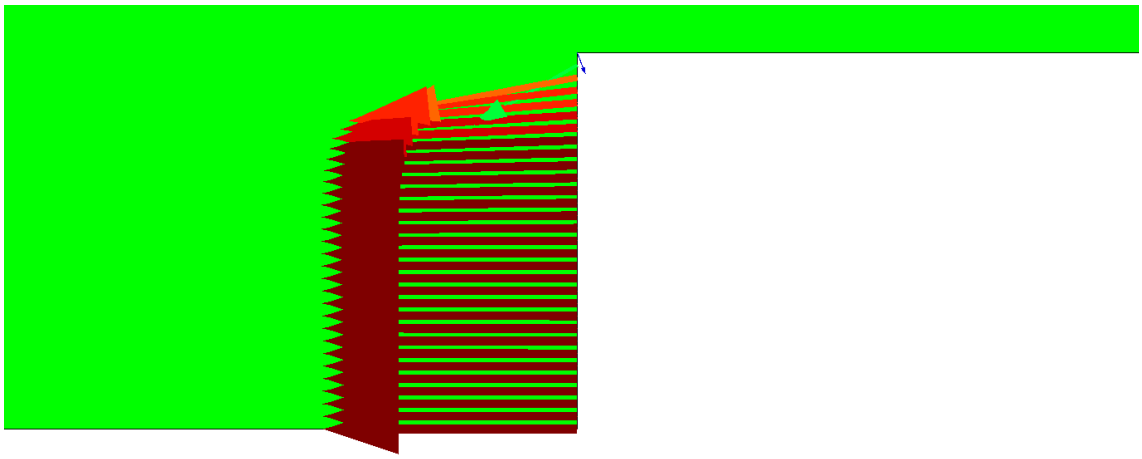

Figure 13 – (a) Velocity field with flow lines that highlight the formation of a vortex near the step face. (b) Pressure field. (c) Traction vectors on the step, generated by the fluid flow.

5.2 Dynamic problems

Flow around a cylinder. The same geometry and boundary conditions of the stationary problem were used, now with a transient formulation. In the pipeline, fluid flow from the left to the right is simulated, passing through a fixed cylinder. The properties of the fluid are the same from the stationary problem; however, the entrance velocity of the flow is elevated so that the graphic results are improved:

$$U_m[m/s] = 1{,}5 \quad e \quad Re = 100 \tag{28}$$

The simulation consists in 1000 time steps $\Delta t = 0{,}01s$, with a total flow time of 10 seconds. The Newwark γ parameter adopted is 0,5 in order for a second order convergence to be obtained.

When the obtained results, presented as follows, are compared with the ones from the stationary simulation, it can be inferred that the flow uniformity and symmetry no longer exist, both for the velocities and the pressures of the fluid (Figura 14 (a) and (b)), as for the tractions caused on the cylinder (Figure 15). The detachment of the vortexes formed after the passage of the flow trough the obstacle can also be observed (Figura 14 (c)).

a)

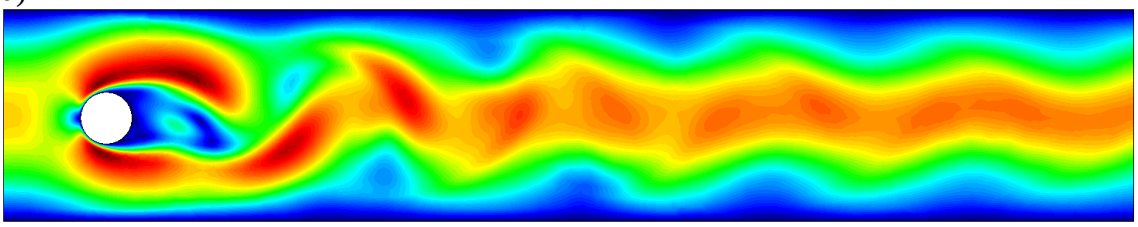

b)

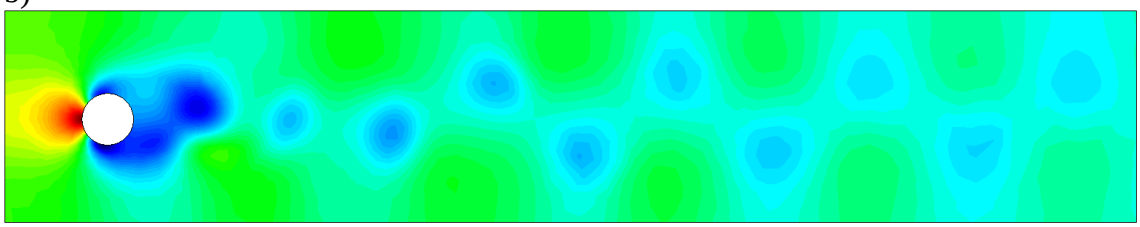

c)

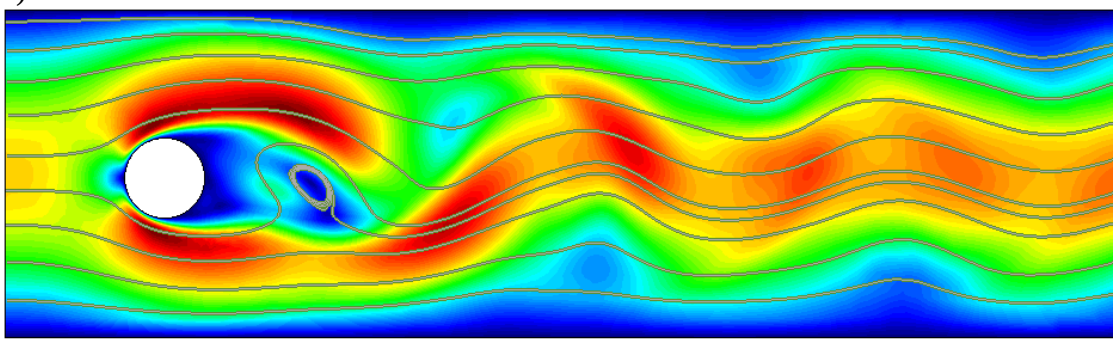

Figura 14 – Flow velocity (a) and pressures (b) fields. The warmer the colors are, the higher are the values. Detail of the velocities field with flow lines (c) highlighting the formation of a vortex after the passage through the cylinder.

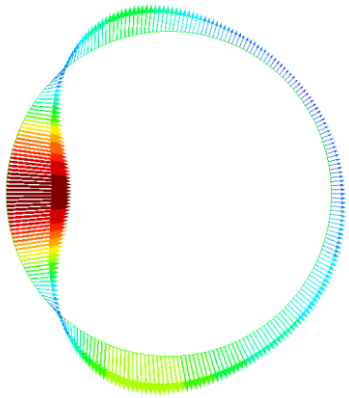

Figure 15 – Traction vectors in the cylinder caused by the flow.

Flow around two consecutive cylinders. Starting from the problem with one cylinder, another cylinder with the same diameter was added, centered in the coordinates (0,9;0,2)m, 0,7m distant from the first cylinder and following the same direction of the pipeline flow. The idea is to observe the influence of the changes generated in the flow by the presence of an obstacle over the other cylinder, and vice versa. The velocities and pressures in the fluid are even more irregular (Figure 16 (a) and (b)) and new points of vortex formation and detaching appear (Figure 16 (c)).

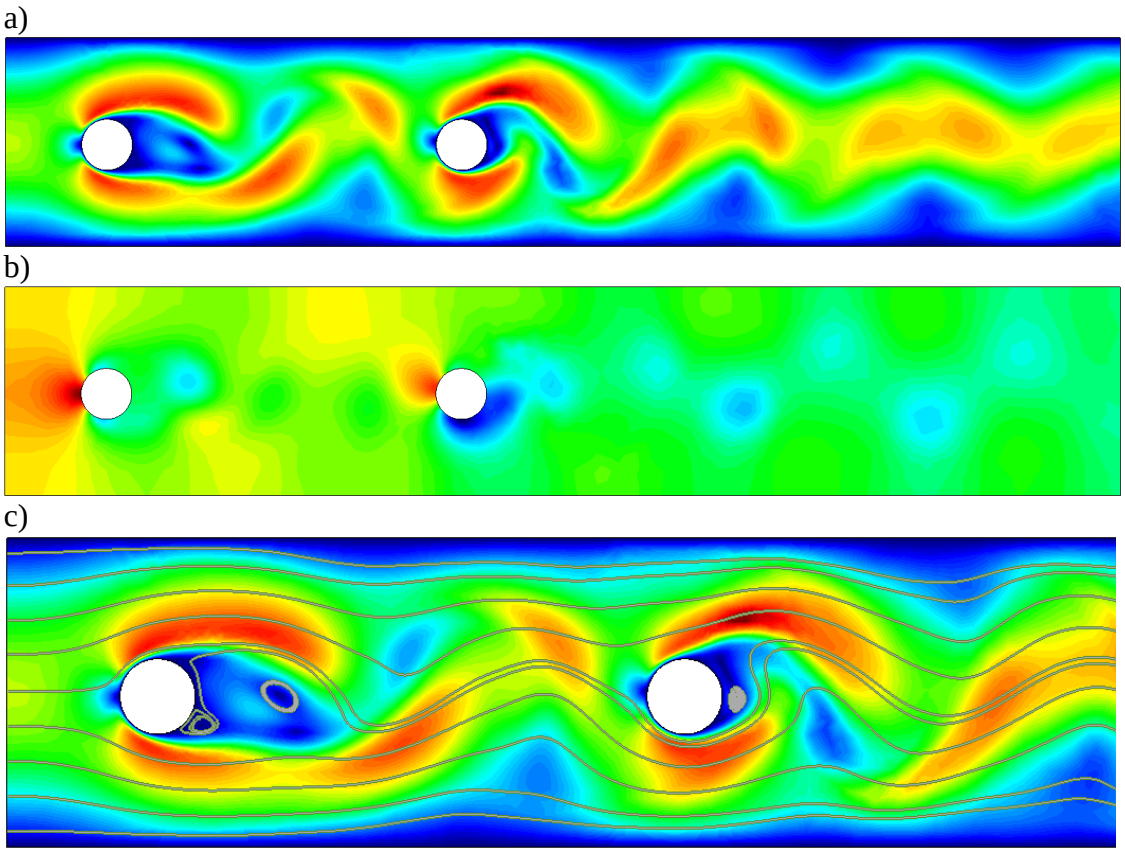

Figure 16 – Flow velocities (a) and pressures (b) fields around two consecutive cylinders. Detail of the velocities field with flow lines (c) highlighting the formation of three vortices after the passage through the obstacles.

By means of the cylinders traction results presented as vectors in Figure 17, the order of magnitude difference for the values obtained in each obstacle is straightforward. The higher traction found in the right cylinder is up to six times higher than the maximum traction in the left cylinder. I.e., in this case, the disturbance in the flow caused by the first obstacle generated a traction increase in the second cylinder.

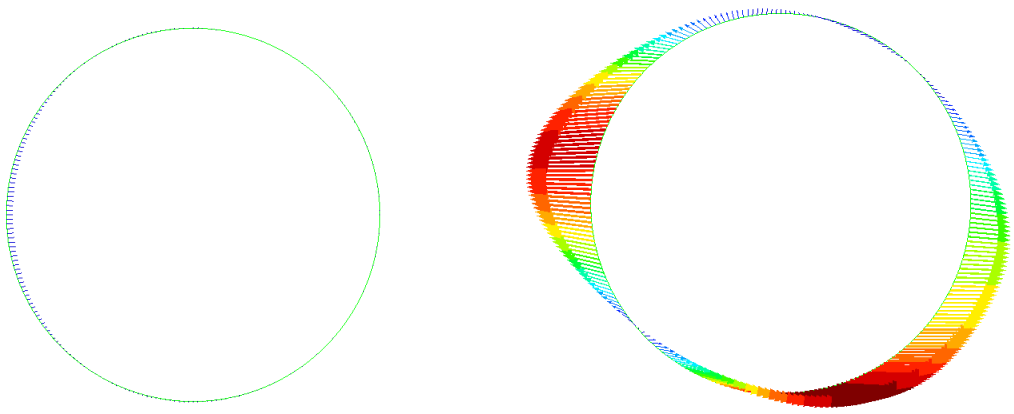

Figure 17 –Vector traction results obtained in the same simulation, maintaining the images proportion so that the magnitudes can be compared.

CONCLUSIONS

This work has presented a study about Fluid-Particle Interaction (FPI), proposing a new manner to simulate problems of this type. For consider the solid grains individually as "structures", this proposition enables to use the formulations and concepts already developed for Fluid-Structure Interaction, adapting the computational code by implementing particle mechanics in the place of structure mechanics for solving dynamic problems of FPI.

The practical part of this research is still in progress, so the results shown above only cover the fluid stationary and dynamic problems. The immersed boundaries and the introduction of particle-particle interaction will be demonstrated in forthcoming publications. Despite this, all the bibliography studied and authors' previous knowledge, who developed the computational programs that are the basis for this work, allows us to believe that the concept is promising and good results will be achieved soon.

ACKNOWLEDGEMENTS

The first author acknowledges scholarship funding from Coordenação de Aperfeiçoamento de Pessoal de Nível Superior (CAPES) to cover some participation in academic activities expenses. All the authors acknowledge Escola Politécnica da Universidade de São Paulo for providing environment and material for scientific development.

REFERENCES

Alder, B. J., and T. E. Wainwright. 1959. "Studies in Molecular Dynamics. I. General Method." *The Journal of Chemical Physics* 31 (2): 459–66. doi:10.1063/1.1730376.

Bićanić, Nenad. 2004. "Discrete Element Methods." In *Encyclopedia of Computational Mechanics*. John Wiley & Sons, Ltd. doi:10.1002/0470091355.ecm006.pub2.

Campello, Eduardo de Morais Barreto. 2016. "Um Modelo Computacional Para O Estudo de Materiais Granulares." http://www.bdpi.usp.br/single.php?_id=002798009.

Campello, Eduardo M. B. 2015. "A Description of Rotations for DEM Models of Particle Systems." *Computational Particle Mechanics* 2 (2): 109–25. doi:10.1007/s40571-015-0041-z.

Crowe, Clayton T., John D. Schwarzkopf, Martin Sommerfeld, and Yutaka Tsuji. 2011. *Multiphase Flows with Droplets and Particles, Second Edition*. CRC Press.

Cundall, P. A., and O. D. L. Strack. 1979. "A Discrete Numerical Model for Granular Assemblies." *Géotechnique* 29 (1): 47–65. doi:10.1680/geot.1979.29.1.47.

Donea, Jean, and Antonio Huerta. 2003. *Finite Element Methods for Flow Problems*. John Wiley & Sons.

Duran, Jacques. 1997. *Sands, Powders, and Grains - An Introduction to the Physics of Granulas Matter*. New York: Springer Science & Business Media. http://www.springer.com/cn/book/9780387986562.

Gerstenberger, Axel, and Wolfgang A. Wall. 2008. "An eXtended Finite Element Method/Lagrange Multiplier Based Approach for Fluid–structure Interaction." *Computer Methods in Applied Mechanics and Engineering*, Computational Methods in Fluid–Structure Interaction, 197 (19): 1699–1714. doi:10.1016/j.cma.2007.07.002.

Gingold, R. A., and J. J. Monaghan. 1977. "Smoothed Particle Hydrodynamics: Theory and Application to Non-Spherical Stars | Monthly Notices of the Royal Astronomical Society | Oxford Academic." https://academic.oup.com/mnras/article/181/3/375/988212/Smoothed-particle-hydrodynamics-theory-and.

Gomes, H. C. 2013. "Método dos elementos finitos com fronteiras imersas aplicado a problemas de dinâmica dos fluidos e interação fluido-estrutura." Text, Universidade de São Paulo. http://www.teses.usp.br/teses/disponiveis/3/3144/tde-26122013-150059/.

Gomes, H. C., and P. M. Pimenta. 2015. "Embedded Interface with Discontinuous Lagrange Multipliers for Fluid–Structure Interaction Analysis." *International Journal for Computational Methods in Engineering Science and Mechanics* 16 (2): 98–111. doi:10.1080/15502287.2015.1009579.

Ibrahimbegovic, Adnan. 1997. "On the Choice of Finite Rotation Parameters." *Computer Methods in Applied Mechanics and Engineering*, Containing papers presented at the Symposium on Advances in Computational Mechanics, 149 (1): 49–71. doi:10.1016/S0045-7825(97)00059-5.

Legay, A., J. Chessa, and T. Belytschko. 2006. "An Eulerian–Lagrangian Method for Fluid–structure Interaction Based on Level Sets." *Computer Methods in Applied Mechanics and Engineering*, Fluid-Structure Interaction, 195 (17): 2070–87. doi:10.1016/j.cma.2005.02.025.

Moës, Nicolas, Eric Béchet, and Matthieu Tourbier. 2006. "Imposing Dirichlet Boundary Conditions in the Extended Finite Element Method." *International Journal for Numerical Methods in Engineering* 67 (12): 1641–69. doi:10.1002/nme.1675.

Neto, Alfredo Gay, and Eduardo M. B. Campello. 2017. "Granular Materials Interacting with Thin Flexible Rods." *Computational Particle Mechanics* 4 (2): 229–47. doi:10.1007/s40571-015-0101-4.

O'Sullivan, Catherine. 2011. *Particulate Discrete Element Modelling: A Geomechanics Perspective*. London ; New York: CRC Press.

Pöschel, Thorsten, and T. Schwager. 2005. *Computational Granular Dynamics: Models and Algorithms*. Springer Science & Business Media.

Rodrigues, Olinde. 1840. "Des lois géométriques qui régissent les déplacements d'un système solid dans l'espace, et de la variation des coordonnées provenant de ces déplacements consideres indépendamment des causes qui peuvent les produire." *Journal de mathématiques pures et appliquées*, 5 edition.

Sawada, Tomohiro, and Akira Tezuka. 2010. "High-Order Gaussian Quadrature in X-FEM with the Lagrange-Multiplier for Fluid–structure Coupling." *International Journal for Numerical Methods in Fluids* 64 (10–12): 1219–39. doi:10.1002/fld.2343.

Wellmann, Christian, and P. Wriggers. 2011. *A Two-Scale Model of Granular Materials Using a Coupled DE-FE Approach*. Univ., Inst. für Kontinuumsmechanik.

Zohdi, T. I. 2007. *An Introduction to Modeling and Simulation of Particulate Flows*. Berkeley: SIAM.

View publication stats